ESKİŞEHİR TECHNICAL UNIVERSITY JOURNAL OF SCIENCE AND TECHNOLOGY A- APPLIED SCIENCES AND ENGINEERING

2019, 20(2), pp. 143 - 152, DOI: 10.18038/aubtda.438120

THE THERMODYNAMIC AND LATTICE VIBRATIONAL PROPERTIES OF CuPd ALLOY UNDER HYDROSTATIC PRESSURE

Sefa KAZANÇ*

Department of Mathematics and Science, Faculty of Education, Fırat University, Elazığ, Turkey

ABSTRACT

In this paper, the effects of hydrostatic pressure on the thermodynamic and vibrational properties such as bulk modulus, second order elastic constants, acoustic phonon frequencies, density of state (DOS) and Grüneisen parameters (γ) on Cu-%20Pd alloys was examined by using the molecular dynamics (MD) simulation. Interaction forces between atoms in the model system were calculated by Quantum Sutton-Chen (Q-SC) potential energy function. The simulation results obtained from this study were compared with the experimental and theoretical results in the literature.

Keywords: Molecular dynamics, Phonon spectra, Quantum Sutton-Chen, Grüneisen parameter

1. INTRODUCTION

The rapid development of technology day by day requires the design and production of new materials. It is very important to know the behaviour of the materials depending on changes of external conditions. Pressure and temperature are two important effects that change the physical and thermodynamic properties of matters. Cu-based inter-metallics have motivated the strong interest in their fundamental properties including interatomic bonding, long range order, crystalline defects, order-disorder transition and diffusion [1-5].This is surprising since CuPd alloys are attracting interest as hydrogen transport membranes [6-11], as materials with good corrosion resistance [12] and as catalysts for the liquid phase reduction of nitrate [13]. CuPd alloys petroleum refining is very important because of its use in important areas such as membranes for hydrogen production and purification [14].

The two most important factors that change phonon frequencies are volume and pressure. The change of phonon frequencies is called anharmonicity [15]. This condition is expressed by the grüneisen parameter (γ). The grüneisen parameter is a valuable quantity in solid-state geophysics because it can be used to set limitations on the pressure and temperature dependence of the thermal properties of the mantle and core, and to constrain the adiabatic temperature gradient [16]. The microscopic description of the grüneisen parameter is based on the vibrational motion of atoms and theoretically is obtained from the differential of the phonon frequency. [17].

The MD simulations are one of the powerful tools used to determine the dynamic properties of materials at atomic scale. The MD simulations has been widely used to study the thermodynamic and structural properties of matter such as intermetallic alloys, polymers and nanostructures [18-21]. In MD simulation, the orbits in the phase space of the particles are determined by numerical integration of the Newton' equations. At high temperature and pressures, the vibrations of atomic systems exhibit anharmonic behaviour. The MD simulations can be modelled the systems exhibiting anharmonic behaviour [17, 22, 23]. The accuracy of the MD simulation results depends on the potential energy function selected for the modelling of the monoatomic or alloy system. One of the potential functions used in MD simulation is EAM [24]. The different versions of EAM are available in literature [25-27]. The SC-EAM is used to investigate the monoatomic and alloy systems [27-29]. This potential function

*Corresponding Author: skazanc@firat.edu.tr
Recieving: 28.06.2018 Accepted: 10.06.2019

is based on the many body interactions. However, the Q-SC potential [28] is given by the same mathematical formula, but the potential parameters used are different.

This study is based on the thermodynamic properties and lattice vibrations of the Cu 20% Pd alloy system and this study was carried out since this type of work has not encountered in the related literature. In this study, we have performed MD simulation using Q-SC potentials to investigate the physical properties of Cu-%20Pd alloy under hydrostatic pressure. We have calculated the pressure dependences of the bulk modulus, C_{11}, C_{12}, C_{44} and density of state for model alloy system. Also, the change of the acoustic phonon frequencies with the pressure was determined. The grüneisen parameter was calculated using the phonon frequency values. The values obtained from the simulation studies were compared with the results in the literature.

2. MATERIALS AND METHODS

The Lagrangian function of the MD cell, which varies in shape and volume proposed by Parrinello and Rahman, is written as follows [30, 31]

$$L_{PR}\left(\mathbf{r}^N, \dot{\mathbf{r}}^N, \mathbf{h}, \dot{\mathbf{h}}\right) = \frac{1}{2}\sum_{i=1}^{N} m_i\left(\dot{\mathbf{s}}_i^t \mathrm{G} \dot{\mathbf{s}}_i\right) - \sum_{i=1}^{N}\sum_{j>i}^{N} \phi\left(\left|\mathbf{h}\mathbf{s}_{ij}\right|\right) + \frac{1}{2} M \mathrm{Tr}\left(\dot{\mathbf{h}}^t \dot{\mathbf{h}}\right) - P_{ext} V \qquad (1)$$

here m_i and s_i are the mass and coordinate of the i*th* atom, respectively. **h** is the tensor containing the MD cell axes, and **G** is the metric tensor. M and P_{ext} are the mass of the MD cell which an arbitrary constant and the pressure externally applied to the system, respectively. The details of the MD calculations can be found in the literature. [32].

In this study, the atoms of the CuPd alloy were placed at the fcc lattice points at the beginning of the simulation. The periodic boundary conditions were applied along the x, y and z axes of the MD cell. The cut-off distance was chosen as $2.2A_{CuCu}$. At the beginning of the simulation, the initial velocities of atoms were randomly determined. The random velocities were produced to fit the Maxwell-Boltzman distribution. The thermostat process was carried out by rescaling the velocities in both MD steps. Both the particles and movement equations of the MD cell were integrated by the Gears' 5th order predictor-corrector algorithm. The MD time step is 4.85 fs. To obtain a stable structure of the alloy system, 50000 time steps were waited at each pressure value. It was seen that the the alloy sytems have stability strcuture at each of pressure values. The acoustic phonon frequencies were calculated by averaging over the last 5000*th* time step.

2.1. The Atomic Interactions

In this work, we modelled the interactions between atoms by using the Q-SC potential. The potential energy of binary alloys in the Q-SC for the systems with *N* atoms is given by;

$$E_T^{SC} = \left\{ \frac{1}{2} \sum_{i^a, j^a}^{N^a} \varepsilon_a \left(\frac{A_a}{r_{ij}} \right)^{n_a} - \sum_{i^a}^{N^a} \varepsilon_a c_a \left[\sum_j \left(\frac{A_a}{r_{ij}} \right)^{m_a} \right]^{1/2} \right\} +$$

$$\left\{ \frac{1}{2} \sum_{i^b, j^b}^{N^b} \varepsilon_b \left(\frac{A_b}{r_{ij}} \right)^{n_b} - \sum_{i^b}^{N^b} \varepsilon_b c_b \left[\sum_j \left(\frac{A_b}{r_{ij}} \right)^{m_b} \right]^{1/2} \right\} + \tag{2}$$

$$\frac{1}{2} \sum_{i^a, j^b}^{N^{ab}} \varepsilon_{ab} \left(\frac{A_{ab}}{r_{ij}} \right)^{n_{ab}} + \frac{1}{2} \sum_{i^b, j^a}^{N^{ba}} \varepsilon_{ba} \left(\frac{A_{ba}}{r_{ij}} \right)^{n_{ba}}$$

where, i^a and i^b indicating summation over type-*a* and type-*b* atoms, respectively. The potential parameters for binary alloy systems can be calculated from mixing rule [18];

$$A_{ij} = A_{ji} = \frac{A_i + A_j}{2}, \quad n_{ij} = n_{ji} = \frac{n_i + n_j}{2}, \quad m_{ij} = m_{ji} = \frac{m_i + m_j}{2} \tag{3}$$

$$\varepsilon_{ij} = \varepsilon_{ji} = \sqrt{\varepsilon_i \, \varepsilon_j} \tag{4}$$

where A is the length parameter; ε is an energy parameter, m and n are integers. The potential parameters for the same and different type atoms of the CuPd alloy have been given in Table 1 [27, 33].

Table 1. Q-SC [28] potential parameters for Cu and Pd

Element	n	m	ε (eV)	c	A (Å)
Cu	10	5	5.7921 x10^{-3}	84.843	3.6030
Pd	12	6	3.2864 x10^{-3}	148.205	3.8813

2.2. Elastic Properties

The elastic constants for the CuPd binary system were calculated using the following formula:

$$C_{ijkm} = -\frac{V_0}{k_B T} \left(\langle P_{ij} P_{km} \rangle - \langle P_{ij} \rangle \langle P_{km} \rangle \right) + \frac{2 N k_B T}{V_0} \left(\delta_{ik} \delta_{jm} + \delta_{im} \delta_{jk} \right) + \langle B1_{ijkm} \rangle + \langle B2_{ijkm} \rangle + \langle B3_{ijkm} \rangle \tag{5}$$

Here the P_{ij} is the stress tensor at the atomic level. The first, second and final terms of equation (5) are the fluctuation, temperature correction and the Born term, respectively. The details of the formulations can be found from literature [34, 35].

The bulk modulus for model system is determined using the following thermodynamic expression:

$$B_m = -V \left(\frac{\partial P}{\partial V} \right)_T \tag{6}$$

2.3. Determination of the Lattice Vibration Frequencies, DOS and Grüneisen Parameter

The solution of the secular equation given in Eq. (7) gives the phonon frequencies of the monoatomic or alloy systems [35, 36].

$$\left|\mathbf{D} - MW^2\mathbf{I}\right| = 0 \tag{7}$$

here **D** is the dynamical matrix of the order ($3n\times3n$), and **I** is the unit matrix. n is the number of atoms in primitive unit cell. The dynamical matrix for the EAM potential function is given as follows [24]:

$$\mathbf{D}(\mathbf{k}) = \sum_j \chi_{0j}(1 - \mathbf{e}^{\mathbf{ik.r}_{0j}}) + F(\rho)^{''}\mathbf{f}^*(\mathbf{k})\mathbf{f}(\mathbf{k}) \tag{8}$$

where

$$\begin{aligned}\chi_{0j} = &\left(\Phi(r_{0j})^{''} + F(\rho)^{'}\rho^a(r_{0j})^{''}\right)\mathbf{r}_{0j}\mathbf{r}_{0j}/(r_{0j})^2 \\ &+ \left(\Phi(r_{0j})^{'} + F(\rho)^{'}\rho^a(r_{0j})^{'}\right)\left(\mathbf{I} - \mathbf{r}_{0j}\mathbf{r}_{0j}/(r_{0j})^2\right)/r_{0j}\end{aligned} \tag{9}$$

$$\mathbf{f}(\mathbf{k}) = \sum_{j\neq0}\rho^a(r_{0j})^{'}(\mathbf{e}^{\mathbf{ik.r}_{0j}})\mathbf{r}_{0j}/r_{0j} \tag{10}$$

$\mathbf{f}^*$ is the complex conjugate of **f** statement, zero is the sub-indice and it shows the selected reference atom [24]. Because of the limited volume effects, the finite atomic distances are used while calculating the dynamic matrix. [37]. The eigenvalues of the dynamic matrix correspond to longitudinal and transverse phonon frequencies. The eigenvalues can be calculated using Jacobi method. The **D** is Hermitian matrix. Eigenvalues can be real and negative. Negative values indicate that the studied system is mechanically unstable. [37].

The density of states are the total number of vibration modes between ω and ω+dω frequencies.

$$g(\omega) = \frac{N_0V}{8\pi^3}\sum_k \delta(\omega - \omega_k) \tag{11}$$

where N_0 is unit cell number and V is unit cell volume.

The Grüneisen parameter is an important quantity in geophysics as it often occurs in equations which describe the thermoelastic behavior of materials at high pressures and temperatures. The Grüneisen parameter varies slowly with the pressure and temperature and it dimensionless. The Grüneisen parameter is an indicator of the anharmonic behaviour. The microscopic definition of the grüneisen parameter can be expressed as the differential of the vibration mode, as follows:

$$\gamma_{i(q)} = -\frac{dln\omega_q}{dlnV} \tag{12}$$

where ω_q is the phonon frequency that is the function of the q-wave vector and V is volume [38].

3. RESULTS AND DISCUSSION

The Cu and Pd atoms of the Cu-%20Pd order alloy system at the starting of simulation were distributed on $L1_2$ type superlattice (with fcc unit cell) sites. The 3200 Cu and 800 Pd atoms (total 4000) were assigned on the fcc lattice points. The centers of fcc structures was occupied by Cu atoms while the corner cites was occupied by Pd atoms. The external pressure of the system was raised from 0 GPa to 50 GPa with 5 GPa increment in each run. At every pressure the MD cell was equilibrated for 50000 time steps to obtain a structurally and thermodynamically stable structure.

Under different pressure values at 300 K, the radial distribution functions (RDF) of the alloy system are shown in Figure 1. The alloy studied was seen to be a fcc structure for all pressure values at the 300 K. In the RDF function vurves, the first peak shows the first neighbours of atoms. At zero pressure, the second peak is 3.698 Å that indicates the lattice parameter. The experimental value of the lattice constant of the Cu-%20Pd alloy was given as 3.675 Å in the literature [39]. The value of the lattice parameter determined from the RDF curve is in agreement with the experimental value. The intensities of the peak of the RDF curves increases with increasing pressure. In addition, as seen from Figure 1, RDF peaks have shifted to the left with the increases of the hydrostatic pressure. The high pressure increases atoms number in the neighbour shell, and so the interatomic distances reduced.

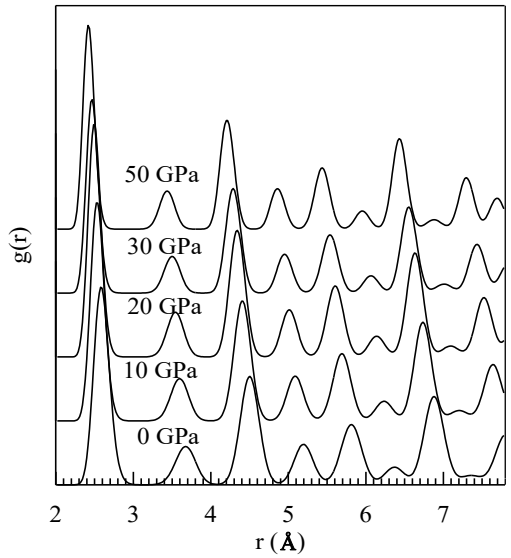

Figure.1 The RDF of CuPd alloy at different pressure values

The change of bulk modulus of the Cu-%20Pd alloy were calculated with increasing pressure in the range 0-50 GPa. The change values of B_m versus P can be seen in Figure 2 for 300 K temperature. The bulk modulus for the model alloy system increases almost linearly with the increasing pressure.

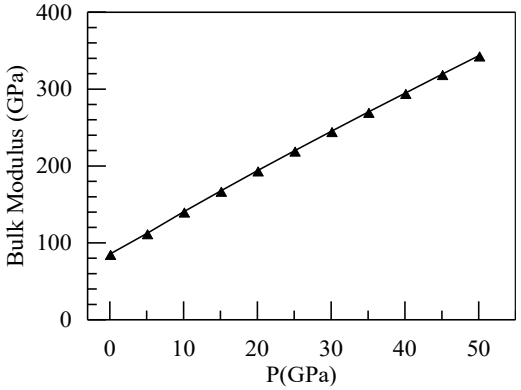

Figure 2. Variation of bulk modulus with pressure for alloy system

One of the parameters, which determine the hardness and stability of materials, is elastic constants. The second order elastic constants were calculated for 300 K temperature at 0–50 GPa with 5 GPa increment. For 300 K, the variance of elastic constants (C11, C12 and C44) with increasing pressure were depicted in Figure 3 and it is seen that from this figure, the elastic constants increases linearly with increasing of pressure. However, it has been observed that the tendency of changes of C_{12} and C_{44} elastic constants are similar, the increase of C_{11} values is more than those of the others. The experimental data of the

elastic constants for alloy system modeled depending on pressure are not available for comparison in the literature.

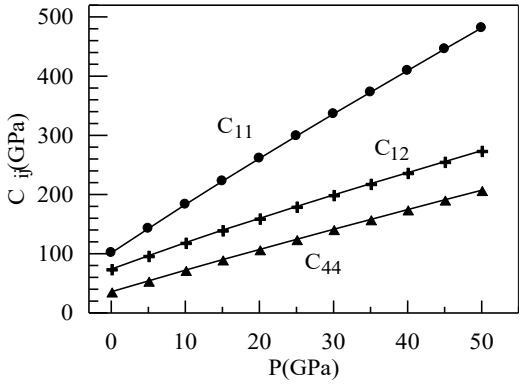

Figure 3. Second order elastic constants as function of pressure

The DOS and the acoustic phonon dispersion curves for the Cu-%20Pd were calculated based on different hydrostatic pressures. The both acoustic phonon spectra and density of states of alloy studied for 300 K at 0 GPa and 50 GPa pressure are shown in Figure 4 (a-b). The dispersion curves for intermediate pressure values shows similar trends. The one longitudinal (L) and two transverse (T_1 and T_2) acoustical branches were observed in Figure 4. Unfortunately, to the knowledge of the author of the present study, there are no experimental studies or theoretical calculations at high pressures for comparison with our results.

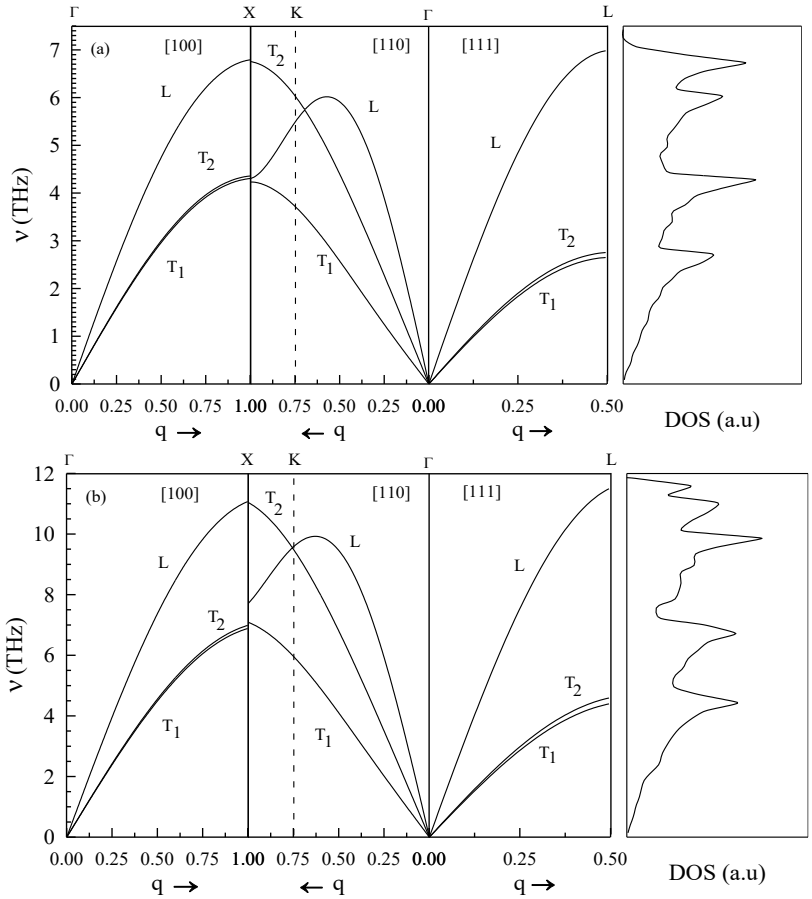

Figure 4. Phonon dispersion curves and density of states of CuPd alloy along high symmetry directions at 300K for a) 0 GPa and b) 50 GPa pressure.

The peaks in the DOS signify the large number of state at the corresponding frequencies [41]. The longitudinal and transverse branches along high symmetry direction are flat away from the zone center. The flat dispersion of the acoustic modes at the Brilliouin boundary gives rise to sharp maximum (see Figure 4) [42].

Figure 5 shows the variation of the phonon frequencies at points X, K and L of the Brillouin zone. From obtained results, it is seen that the acoustic phonon frequencies increase with the increasing pressure. Generally, the application of hydrostatic pressure increases the phonon frequency because of the increasing stiffening of the interatomic interactions [40].

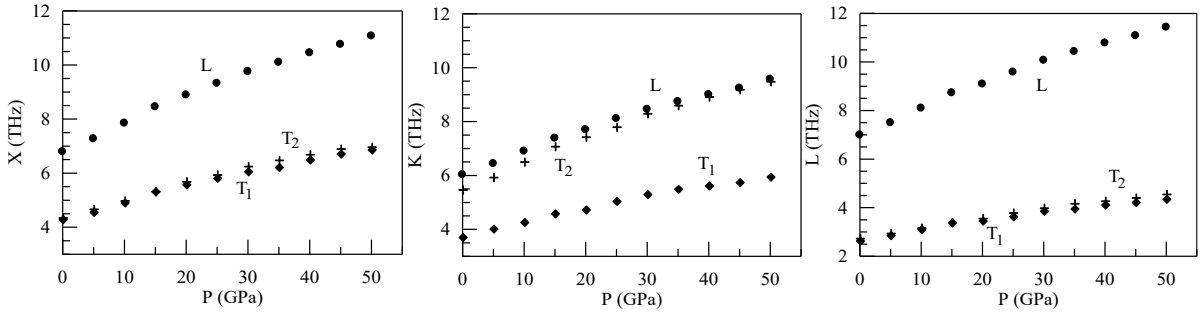

Figure 5. Variations of acoustic phonon frequencies with pressure for 300 K at X, K and L points of Brillouin zone

In Figure 6 shows the vibration density of states at 0, 10, 20, 30 40 and 50 GPa hydrostatic pressure values. As seen from that Figure, the peaks of density of states are shifting to the right with increasing pressure value. Also, the intensities of the peaks of the density of states increase with increasing pressure.

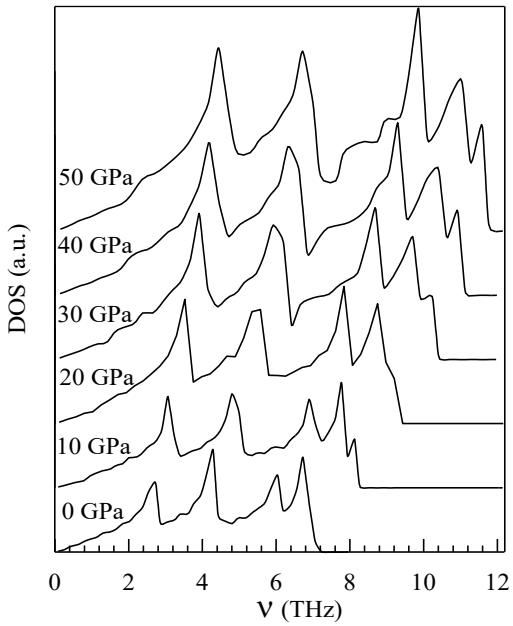

Figure 6. Variations of phonon density of states with increasing pressures

The phonon frequencies do not depend on volume in perfectly harmonic lattice. The variation of phonon frequency with temperature and pressure variation is known to occur due to anharmonicity of the interatomic potential [15, 17]. The change of phonon spectra with pressure for model alloy system studied is used for calculation of the Grüneisen parameter. The Grüneisen parameters have been calculated at X, K and L point of Brilliouin zone for 300 K, 500 K and 800 K temperature values using

the acoustic phonon frequencies. The Grüneisen parameters of acoustic vibration modes for each branch are listed in Table 2.

Table 2. Calculated grüneisen parameters of the acoustic vibration modes at the X, K and L point of the primitive cell

T(K)	[100] direction (X point)			[110] direction (K point)			[111] direction (L point)		
	γ_L	γ_{T1}	γ_{T2}	γ_L	γ_{T1}	γ_{T2}	γ_L	γ_{T1}	γ_{T2}
300	1.894	1.826	1.880	1.759	1.759	2.120	1.899	1.928	1.893
500	1.925	1.939	1.906	1.763	1.808	2.163	1.921	1.948	1.910
800	1.947	1.952	1.978	1.788	1.813	2.201	1.929	1.951	1.932

In the literature, the experimental measurements or theoretical calculations were not encountered to compare our results. As it is seen from obtained results, the Grüneisen parameters have increased with the increasing temperature. In studies made for different alloy systems were observed that the Grüneisen parameter increases with the increasing temperature and obtanied results are compatible with the literature [43, 44].

REFERENCES

[1] Shah V, Yang L. Nanometre fcc clusters versus bulk bcc alloy: the structure of Cu-Pd catalysts. Philosophical Magazine A 1999; 79: 2025-2049.

[2] Wang X, Ludwig K.F, Malis O, Mainville J. Temperature dependence of the diffuse-scattering fine structure in Cu-Pd alloys. Physical Review B 2001; 63: 1-4.

[3] Kamakoti P, Sholl D.S. A comparison of hydrogen diffusivities in Pd and CuPd alloys using density functional theory. Journal of Membrane Science 2003; 225: 145-154.

[4] Kamakoti P, Sholl D.S. Ab initio lattice-gas modeling of interstitial hydrogen diffusion in CuPd alloys. Physical Review B 2005; 71: 1-9.

[5] Wu E.J, Ceder G. Using bond-length-dependent transferable force constants to predict vibrational entropies in Au-Cu, Au-Pd, and Cu-Pd alloys. Physical Review B 2003; 67: 1-7.

[6] Rao F, Way JD, McCormick Rl, Paglieri SN. Preparation and characterization of Pd-Cu composite membranes for hydrogen separation. Chem Eng J 2003; 93: 11-22.

[7] Pan X.L, Kilgus M, Goldbach A. Low-Temperature H_2 and N_2 Transport Through Thin $Pd_{66}Cu_{34}H_x$ Layers. Catal Today 2005; 104: 225-230.

[8] Morreale BD, Howard BH, Iyoha O, Enick RM, Ling C, Sholl DS. Experimental and computational prediction of the hydrogen transport properties of Pd_4S. Ind Eng Chem Res 2007; 46 (19): 6313-6319.

[9] O' Brien CP, Howard BH, Miller JB, Morreale BD, Gellman AJ. Inhibition of hydrogen transport through Pd and $Pd_{47}Cu_{53}$ membranes by H_2S at 350 C. J Membr Sci 2010; 349 (1–2): 380-384.

[10] Peters T, Kaleta T, Stange M, Bredesen R. Development of thin binary and ternary Pd-based alloy membranes for use in hydrogen production. J Membr Sci 2011; 383 (1–2): 124-134.

[11] Sharma R, Sharma Y. Hydrogen permeance studies in ordered ternary Cu-Pd alloys. International Journal of Hydrogen Energy 2015; 40: 14885-14899.

[12] Volkov AY. Improvements to the Microstructure and Physical Properties of Pd-Cu-Ag Alloys. Platinum Met Rev 2004; 48: 3-12.

[13] Pintar A. Catalytic processes for the purification of drinking water and industrial effluents. Catal Today 2003; 77: 451-465.

[14] Kart SÖ, Erbay A, Kılıç H, Cagin T, Tomak M. Molecular dynamics study of Cu-Pd ordered alloys. Journal of Achievements in Materials and Manufacturing Engineering 2008; 31(1): 41-46.

[15] Wei L, Wang XP, Liu B, Zhang YY, Lu XS, Yang YG, Zhang HJ and Zhao X. The role of acoustic phonon anharmonicity in determining thermal conductivity of $CdSiP_2$ and $AgGaS_2$: First principles calculations. Aip Advances 2015; 5: 127236.

[16] Vocadlo NL and Price GD. The grüneisen parameter-computer calculations via lattice dynamics. Physics of the Earth and Planetary Interiors 1994; 82: 261-270.

[17] Mittal R, Gupta MK, Chaplot SL. Phonons and anomalous thermal expansion behaviour in crystalline solids. Progress in Materials Science 2018; 92: 360–445.

[18] Cagin T, Dereli G, Uludogan M and Tomak M. Thermal and mechanical properties of some fcc transition metals. Physical Review B 1999; 59(4): 3468-3472.

[19] Zhang XJ and Chen CL. Phonon dispersion in the fcc metals Ca, Sr and Yb. J Low Temp Phys 2012; 169: 40-50.

[20] Tolpin KA, Bachurin VI and Yurasova VE. Features of energy dependence of NiPd sputtering for various ion irradiation angles. Nucl Instrum Methods Phys Res B 2012; 273: 76-79.

[21] Louail L, Maouche D, Roumili A and Hachemi A. Pressure effect on elastic constants of some transition metals. Mat Chem Phys 2005; 91: 17-20.

[22] Marque´s LA, Pelaz L, Aboy M, Lopez P, Barbolla J. Atomistic modelling of dopant implantation and annealing in Si: damage evolution, dopant diffusion and activation. Comput Mat Sci 2005; 33: 92-105.

[23] Shao Y, Clapp PC, Rifkin JA. Molecular dynamics simulation of martensitic transformations in NiAl. Metall Mater Trans A 1996; 27A: 1477-1489.

[24] Daw MS, Hatcher RD. Application of the embedded atom method to phonons in transition metals. Solid State Comm 1985; 56: 697-699.

[25] Voter AF, Chen SP. Accurate Interatomic Potentials for Ni, Al, and Ni_3Al. Mat Res Soc Symp Proc 1987; 82: 175.

[26] Finnis MW and Sinclair JE. A simple empirical N-body potential for transition metals. Philosophical Magazine 1984; 50: 45-55.

[27] Sutton AP, Chen J. Long-range Finnis-Sinclair potentials. J Philosophical Magazine Letter 1990; 61: 139-146.

[28] Grujicic M, Dang P. Computer simulation of martensitic transformation in Fe-Ni face-centerd cubic alloys. Materials Science and Engineering A 1995; 201: 194-204.

[29] Gui J, Cui Y, Xu S, Wang Q, Ye Y, Xiang M, Wang R. Embedded- atom method study of the effect of order degree on the lattice parameters of Cu based shape-memory alloys. J Phys Condens Matter 1994; 6: 4601-4614.

[30] Parrinello M and Rahman A. Crystal Structure and Pair Potentials: A Molecular-Dynamics Study. Phys Rev Lett 1980; 45: 1196-1201.

[31] Parrinello M and Rahman A. Polymorphic transitions in single crystals: A new molecular dynamics method. J Appl Phys 1981; 52: 7182-7190.

[32] Kazanc S, Ozgen S, Adiguzel O. Pressure effects on martensitic transformation under quenching process in a molecular dynamics model of NiAl alloy. Physica B 2003; 334: 375-381.

[33] Çagin T, Qi Y, Li H, Kimura Y, Ikeda H, Johnson W.L, Goddard III W.A. The quantum Sutton-Chen many-body potential for properties of fcc metals. MRS Symposium Ser 1999; 554: 43.

[34] Wolf R.J, Mansour K.A, Lee M.W and Ray J.R. Temperature dependence of elastic constants of embedded-atom models of palladium. Physical Review B 1992; 46: 8027-8035.

[35] Karimi M, Stapay G, Kaplan T and Mostoller M. Temperature dependence of the elastic constants of Ni: reliability of EAM in predicting thermal properties. Modelling Simul Mater Sci Eng 1997; 5: 337-346.

[36] Haas H, Wang CZ, Ho KM, Fahnle M and Elsasser C. Temperature dependence of the phonon frequencies of molybdenum: a tight-binding molecular dynamics study. J Phys Condens Matter 1999; 11: 5455-5462.

[37] Kong LT. Phonon dispersion measured directly from molecular dynamics simulations. Computer Physics Communications 2011; 182: 2201-2207.

[38] Vocadlo L, Poirer JP and Price GD. Grüneisen parameters and isothermal equations of state. American Mineralogist. 2000; 85: 187-193.

[39] Subramanian PR and Laughlin DE. Phase diagram Evaluations: Section II. Journal of Phase Equilibrian 1991;12(2): 231-243.

[40] Kazanc S, Ciftci YO, Colakoglu K, Ozgen S. Temperature and pressure dependence of the some elastic and lattice dynamical properties of copper: a molecular dynamics study. Physica B 2006; 381: 96–102.

[41] Dahal S, Kafle G, Kaphle GC and Adhikari NP. Study of Electronic and Magnetic Properties of CuPd, CuPt, Cu_3Pd and Cu_3Pt: Tight Binding Linear Muffin-Tin Orbitals Approach. Journal of Institute of Science and Technology 2014; 19(1): 137-144.

[42] Brüesch P. Phonon: Theory and Experiments I, Springer Series in Solid State Sciences 34, New York, 1982, pp. 84-85.

[43] Körözlü N. Basic Physical Properties Calculations of $Cd_xZn_{1-x}X$(X=Te, Se, S) Alloys and WP, GdX (X=Bi, Sb) Compounds with Methods Based on Denstiy Functional Theory (DFT). PhD, Gazi University, Ankara, Turkey, 2009.

[44] Sürücü G. The Investigation of the Structural, Elastic, Thermodynamic and Vibrational Properties of Some A_3B (L_{12}) Type Alloys Using Ab Initio Method. MSc, Gazi University, Ankara, Turkey, 2009.